

# TRANSVERSE MOMENTUM SPECTRA OF D- AND B-MESONS IN HADRON COLLISIONS AT HIGH ENERGIES

G. I. Lykasov<sup>a</sup>, Z. M. Karpova<sup>a</sup>, M.N.Sergeenko<sup>b</sup> and V. A. Bednyakov<sup>a</sup>

*for the ATLAS Collaboration*

<sup>a</sup>Joint Institute for Nuclear Research  
Dubna 141980, Moscow region, Russia

<sup>b</sup>Belarus State Transport University, Gomel, Belarus

E-mail: lykasov@jinr.ru; zkarpova@jinr.ru; Vadim.Bednyakov@jinr.ru

Transverse momentum spectra of charmed and beauty mesons produced in proton-proton and proton-antiproton collisions at high energies are analyzed within the modified quark-gluon string model (QGSM). We got a satisfactory description of the experimental data on  $p_t$  spectra of  $D$ - and  $B$ -mesons produced in the  $p-\bar{p}$  collisions which were obtained by the CDF Collaboration at the Tevatron at  $1.5(GeV/c) < p_t < 20(GeV/c)$ . Our results are similar to the calculations within the NLO of QCD at  $p_t > 6(GeV/c)$ , which have a big uncertainty, except for the kinematic region of very high  $p_t$ , where  $p_t > 20.(GeV/c)$ . It can be due to the contribution of gluons inside the colliding proton and antiproton which can interact with other gluons and quarks(antiquarks) and fragmentate to charmed mesons. This effect is not included in the presented QGSM. The results show that the QGSM can be used to analyze transverse momentum spectra of charmed and beauty mesons produced both in  $p-p$  and  $p-\bar{p}$  collisions at very high energies up to the LHC energies. We compare also our predictions for the LHC with the calculations on the charm and beauty quark production in  $p-p$  collision obtained within the NLO QCD by the ALICE Collaboration.

## 1 Introduction

Various approaches of perturbative QCD including the next-to-leading order calculations (NLO QCD) have been applied to construct distributions of quarks in a proton. The

theoretical analysis of the lepton deep inelastic scattering (DIS) off protons and nuclei provides rather realistic information on the distribution of light quarks like  $u, d, s$  in a proton. However, to find a believable distribution of heavy quarks like  $c(\bar{c})$  and especially  $b(\bar{b})$  in a proton describing the experimental data on the DIS is a non-trivial task. It is mainly due to small values of  $D$ - and  $B$ - meson yields in the DIS at existing energies. Even at the Tevatron energies the  $B$ - meson yield is not so large. At LHC energies the multiplicity of  $D$ - and  $B$ - mesons produced in  $p-p$  collisions will be significantly larger. Therefore one can try to extract a new information on the distribution of these heavy mesons in a proton. In this paper we suggest to study the distribution of heavy quarks like  $c(\bar{c})$  and  $b(\bar{b})$  in a proton from the analysis of the future LHC experimental data.

The multiple hadron production in hadron-nucleon collisions at high initial energies and large transfers is usually analyzed within the hard parton scattering model (HPSM) suggested in Refs.[1]. The HPSM is significantly improved by applying the QCD parton approach implemented in the modified minimal-subtraction renormalization and factorization scheme. It provides a rigorous theoretical framework for a global data analysis [2, 3]; however, it has some uncertainties related to different scale parameters.

## 2 General formalism

In this paper we analyze the  $D$ -meson production in the  $p-p$  and  $p-\bar{p}$  collisions within the QGSM [4, 5] including the transverse motion of quarks and diquarks in colliding protons [6]. As is known, the cylinder type graphs for the  $p-p$  collision presented in Fig.1 make the main contribution to this process [4]. A physical meaning of the graph presented in Fig.1 is the following. The left diagram of Fig.1, the so-called one-cylinder graph, corresponds to the case where two colorless strings are formed between the quark/diquark ( $q/qq$ ) and the diquark/quark ( $qq/q$ ) in colliding protons; then, after their breakup,  $q\bar{q}$  pairs are created and fragmented to a hadron, for example,  $D$ -meson. The right diagram of Fig.1, the so-called multicylinder graph, corresponds to creation of the same two colorless strings and many strings between sea quarks/antiquarks  $q/\bar{q}$  and sea antiquarks/quarks  $\bar{q}/q$  in the colliding protons. The general form for the invariant inclusive hadron spectrum within the QGSM is [5, 6]

$$E \frac{d\sigma}{d^3\mathbf{p}} \equiv \frac{2E^*}{\pi\sqrt{s}} \frac{d\sigma}{dx dp_t^2} = \sum_{n=1}^{\infty} \sigma_n(s) \phi_n(x, p_t) , \quad (1)$$

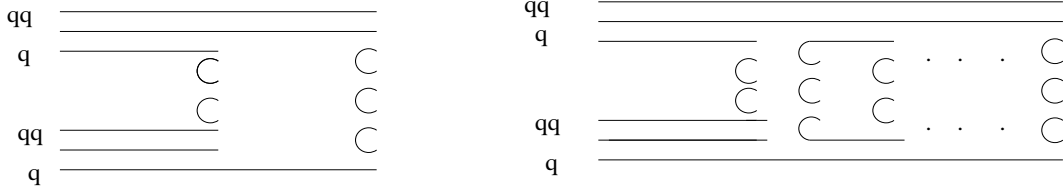


Figure 1: The one-cylinder graph (left diagram) and the multi-cylinder graph (right diagram) for the inclusive  $pp \rightarrow hX$  process.

where  $E, \mathbf{p}$  are the energy and the three-momentum of the produced hadron  $h$  in the l.s. of colliding protons,  $E^*, s$  are the energy of  $h$  and the square of the initial energy in the c.m.s of  $p - p$ ,  $x, p_t$  are the Feynman variable and the transverse momentum of  $h$ ;  $\sigma_n$  is the cross section for production of the  $n$ -Pomeron chain (or  $2n$  quark-antiquark strings) decaying into hadrons, calculated within the “eikonal approximation” [7], the function  $\phi_n(x, p_t)$  has the following form [6]:

$$\phi_n(x, p_t) = \int_{x^+}^1 dx_1 \int_{x_-}^1 dx_2 \psi_n(x, p_t; x_1, x_2) , \quad (2)$$

where

$$\begin{aligned} \psi_n(x, p_t; x_1, x_2) = & F_{qq}^{(n)}(x_+, p_t; x_1) F_{q_v}^{(n)}(x_-, p_t; x_2) / F_{q_v}^{(n)}(0, p_t) + \\ & + F_{q_v}^{(n)}(x_+, p_t; x_1) F_{qq}^{(n)}(x_-, p_t; x_2) / F_{qq}^{(n)}(0, p_t) + \\ & 2(n-1) F_{q_s}^{(n)}(x_+, p_t; x_1) F_{q_s}^{(n)}(x_-, p_t; x_2) / F_{q_s}^{(n)}(0, p_t) . \end{aligned} \quad (3)$$

and  $x_{\pm} = 0.5(\sqrt{x^2 + x_t^2} \pm x)$ ,  $x_t = 2\sqrt{(m_h^2 + p_t^2)}/s$ ,

$$F_{\tau}^{(n)}(x_{\pm}, p_t; x_{1,2}) = \int d^2 k_t \tilde{f}_{\tau}^{(n)}(x_{1,2}, k_t) \tilde{G}_{\tau \rightarrow h} \left( \frac{x_{\pm}}{x_{1,2}}, k_t; p_t \right) , \quad (4)$$

$$F_{\tau}^{(n)}(0, p_t) = \int_0^1 dx' d^2 k_t \tilde{f}_{\tau}^{(n)}(x', k_t) \tilde{G}_{\tau \rightarrow h}(0, p_t) = \tilde{G}_{\tau \rightarrow h}(0, p_t) . \quad (5)$$

Here  $\tau$  means the flavor of the valence (or sea) quark or diquark,  $\tilde{f}_{\tau}^{(n)}(x', k_t)$  is the quark distribution function depending on the longitudinal momentum fraction  $x'$  and the transverse momentum  $k_t$  in the  $n$ -Pomeron chain;  $\tilde{G}_{\tau \rightarrow h}(z, k_t; p_t) = z \tilde{D}_{\tau \rightarrow h}(z, k_t; p_t)$ ,

$\tilde{D}_{\tau \rightarrow h}(z, k_t; p_t)$  is the fragmentation function of a quark (antiquark) or diquark of flavor  $\tau$  into a hadron  $h$  ( $D$ -meson in our case). We present the quark distribution in a proton in the factorized form  $\tilde{f}_\tau(x, k_t) = f_\tau(x)g_\tau(k_t)$ . After the integration of Eq.(4) over  $d^2k_t$  according to [6], we have

$$F_\tau^{(n)}(x_\pm, p_t; x_{1,2}) = \tilde{f}_\tau^{(n)}(x_{1,2})G_{\tau \rightarrow h}(z)I_n(z, p_t) , \quad (6)$$

where  $z = x_\pm/x_{1,2}$ ,  $I_n(z, p_t) = B_z^2/(2\pi(1 + B_z m_D)) \exp(-B_z(m_{Dt} - m_D))$ ,  $m_{Dt}^2 = p_t^2 + m_D^2$ ;  $B_z = B_0/(1 + n\rho z^2)$ ,  $\rho$  is the ratio of the slopes for the quark distribution and fragmentation function as a function of  $k_t$  [6]. We calculated the differential cross section  $d\sigma/dp_t^2$  for  $D$ -mesons produced in  $p - p$  collisions at the energy  $\sqrt{s} = 27.4 \text{ GeV}$  and compare with the existing experimental data [8]

$$\frac{d\sigma}{dp_t^2} = \frac{\pi}{2} \sqrt{s} \sum_{n=0}^{\infty} \sigma_n(s) \int \phi_n(x, p_t) \frac{dx}{E^*} . \quad (7)$$

As is mentioned in the Introduction, the production of heavy mesons like  $D$ - and  $B$ -mesons in proton-antiproton collisions at high energies is usually analyzed within the different schemes of QCD. To study these processes within the QGSM we have to include at least one additional graph corresponding to the creation of three chains between quarks in the initial proton and antiquarks in the colliding antiproton, as is illustrated in Fig.2 (bottom diagram). The left and right diagrams in Fig.2 are similar to the one-cylinder and multicylinder diagrams for the  $p - p$  collision in Fig.1 with a following difference. In the  $p - \bar{p}$  collision two colorless strings between quark/diquark ( $q/qq$ ) in the initial proton and antiquark/antidiquark ( $\bar{q}/\bar{q}q$ ) are created. Many quark-antiquark ( $q - \bar{q}$ ) strings for  $p - \bar{p}$  collision ( Fig.2, right diagram) are the same as for the  $p - p$  collision ( Fig.1, right diagram). Therefore, the invariant inclusive spectrum of hadrons produced in the  $p - \bar{p}$  collision calculated within the QGSM has the following form:

$$E \frac{d\sigma^{p\bar{p}}}{d^3\mathbf{p}} = (1 - \omega) \sum_{n=0}^{\infty} \sigma_n(s) \phi_n^{p\bar{p}}(x, p_t) + \omega \tilde{\phi}(x, p_t) , \quad (8)$$

where  $1 - \omega$  is the probability of contribution of the cut one-cylinder (one-Pomeron exchange) and cut multicylinder (multi-Pomeron exchanges) graphs presented in the left and right diagrams of Fig.2, whereas  $\omega$  is the probability of the contribution of the three-chain diagram in Fig.2 to the inclusive spectrum. The value of  $\omega$  can be estimated as the ratio of the  $p - \bar{p}$  annihilation cross section  $\sigma_{p-\bar{p}}^{ann}$  to the total  $p - \bar{p}$  cross section

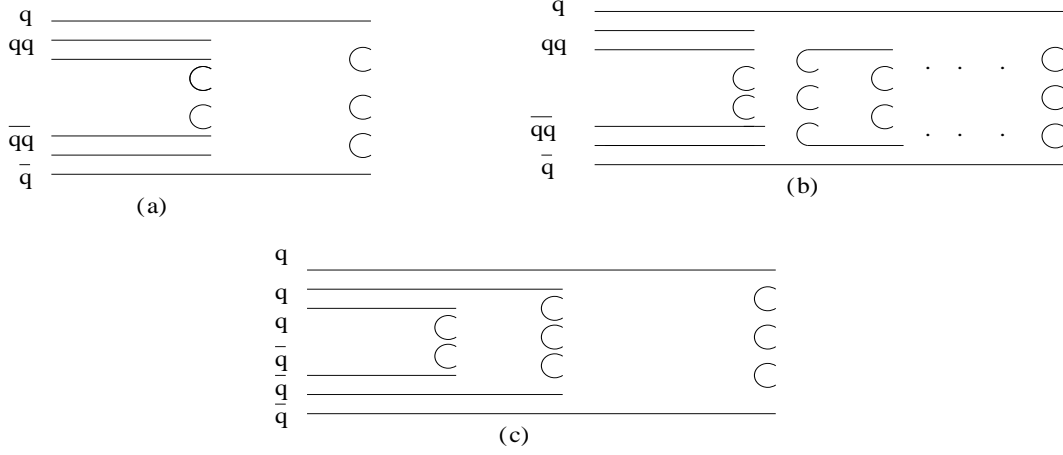


Figure 2: The one-cylinder graph (left diagram), the multicylinder graph (right diagram), and the three-chain graph (bottom diagram) for the  $p\bar{p} \rightarrow hX$  inclusive process.

$\sigma_{p-\bar{p}}^{tot}$ . The cross section  $\sigma_{p-\bar{p}}^{tot}$  is well known in the wide range of the initial energies to the Tevatron energy, whereas experimental data on  $\sigma_{p-\bar{p}}^{ann}$  are available only for the antiproton initial energy about 10 GeV, see [9] and references therein. However, some theoretical predictions, see for example [10, 11], show that asymptotically  $\sigma_{p-\bar{p}}^{ann}$  goes to about 2 – 4 mb. It corresponds to  $\omega \simeq \sigma_{p-\bar{p}}^{ann}/\sigma_{p-\bar{p}}^{tot} < 0.1$  at the Tevatron energy.

The form for the function  $\phi_n^{p\bar{p}}(x, p_t)$  is similar to  $\phi_n(x, p_t)$  entering into Eq.(3) by replacing  $F_{q_v}^{(n)}(x_-, p_t; x_2)$ ,  $F_{q_v}^{(n)}(0, p_t)$  to  $F_{\bar{q}\bar{q}}^{(n)}(x_-, p_t; x_2)$ ,  $F_{\bar{q}\bar{q}}^{(n)}(0, p_t)$  respectively, and replacing  $F_{q\bar{q}}^{(n)}(x_-, p_t; x_2)$ ,  $F_{q\bar{q}}^{(n)}(0, p_t)$  to  $F_{\bar{q}}^{(n)}(x_-, p_t; x_2)$  and  $F_{\bar{q}}^{(n)}(0, p_t)$  respectively. The additional term  $\tilde{\phi}(x, p_t)$  entering into Eq.(8) has the following form

$$\tilde{\phi}(x, p_t) = 3\tilde{F}_{q_v}(x_+, p_t)\tilde{F}_{\bar{q}_v}(x_-, p_t)/\tilde{F}_q(0, p_t) , \quad (9)$$

where  $\tilde{F}_{q_v(\bar{q}_v)}(x_{\pm}, p_t) = F_{q_v(\bar{q}_v)}^{(n=1)}(x_{\pm}, p_t)$  and  $\tilde{F}_q(0, p_t) = F_q^{(n=1)}(0, p - t)$ .

### 3 Results and discussion

To illustrate our approach we present in Fig.3 the inclusive spectrum  $d\sigma/dp_t^2$  of  $D^0$ -mesons produced in the reaction  $pp \rightarrow D^0X$  at  $\sqrt{s} = 27.4$  GeV as a function of  $p_t^2$ . One can see from Fig.3 that the use of different values for the intercept  $\alpha_{\Psi}(0)$  leads mainly to

the shift of the theoretical lines along the  $y$  axis. One can see a satisfactory description of the experimental data at both values for the linear  $\Psi$ -trajectory when  $\alpha_\Psi(0) = -2.18$  and for the nonlinear one when  $\alpha_\Psi(0) = 0$ . Unfortunately, the experimental data are very poor because of big error bars; therefore, we cannot get new information on the  $\Psi$ -trajectory.

The inclusive  $p_t$  spectra of  $D^0$ - and  $B^+$ -mesons produced in the  $p - \bar{p}$  collision at the Tevatron energy are presented in Fig.4. One can see rather satisfactory description of the experimental data [12] for  $D^0$ - and  $B^+$ -mesons using  $\omega = 0.1$  and  $B_0 = 0.65$  for  $D$ -mesons, and  $B_0 = 0.55$  for  $B$ -mesons,  $\lambda = 2\alpha'_{D^*(B^*)}(0) \langle p_t^2 \rangle$ ,  $\alpha'_{D^*(B^*)}(0) \simeq 0.5(\text{GeV}/c)^{-2}$  is the slope of the  $D^*$ - or  $B^*$ - Regge trajectory  $\langle p_t^2 \rangle$  is the mean transverse momentum squared of the  $D$ -meson or  $B$ -meson. One can see that to describe the experimental data on  $p_t$  spectra of the meson produced in  $p - \bar{p}$  collisions at very high energies and big values for  $p_t$  within the QGSM we cannot include the three-chain graph (Fig.2c). The predictions for inclusive  $p_t$  spectra of  $D^0$ - and  $B^+$ -mesons produced in the  $p - p$  collision at LHC energies and the NLO QCD calculation for the produced charmed quarks [13] are presented in Fig.5

#### 4 Conclusion

In conclusion we have shown that the modified QGSM including the intrinsic longitudinal and transverse motion of quarks (antiquarks) and diquarks in colliding protons allowed us to describe rather satisfactory the existing experimental data on inclusive spectra of  $D$ - mesons produced in  $p - p$  collisions and to make some predictions for similar spectra at LHC energies. To verify whether these predictions can be believable or not we apply the QGSM to the analysis of charmed and beauty meson production in proton-antiproton collisions at Tevatron energies including graphs of like those in Fig.2c corresponding to annihilation of quarks and antiquarks in colliding  $p$  and  $\bar{p}$  and production of  $D$ -mesons. We got a satisfactory description of the experimental data on  $p_t$  spectra of  $D^0$ - and  $B^+$ -mesons produced in the  $p - \bar{p}$  collisions which were obtained by the CDF Collaboration at the Tevatron [12] at  $6.(\text{GeV}/c) \leq p_t \leq 12.(\text{GeV}/c)$ . Our results are similar to the calculations within the NLO of QCD [2, 3] except for the kinematic region of very high  $p_t$  where  $p_t > 20.(\text{GeV}/c)$ . It can be due to the contribution of gluons inside the colliding proton and antiproton which can interact with other gluons and quarks(antiquarks) and fragmentate to charmed mesons. This effect is not included in the presented QGSM. Therefore, as the next step in the analysis of this process within the QGSM we intend

to include this contribution. The results show that the QGSM can be used to analyze transverse momentum spectra of charmed mesons produced both in  $p - p$  and  $p - \bar{p}$  collisions at very high energies up to the LHC energies. We found that the  $p_t$  spectra of  $D$ - and  $B$ -mesons calculated within the QGSM are almost insensitive to the form of the sea  $c(\bar{c})$  and  $b(\bar{b})$  quark distributions in colliding protons/antiprotons. To find a new information on it we intend to study the charm and beauty hadron production in  $p - p$  collisions at small scattering angles.

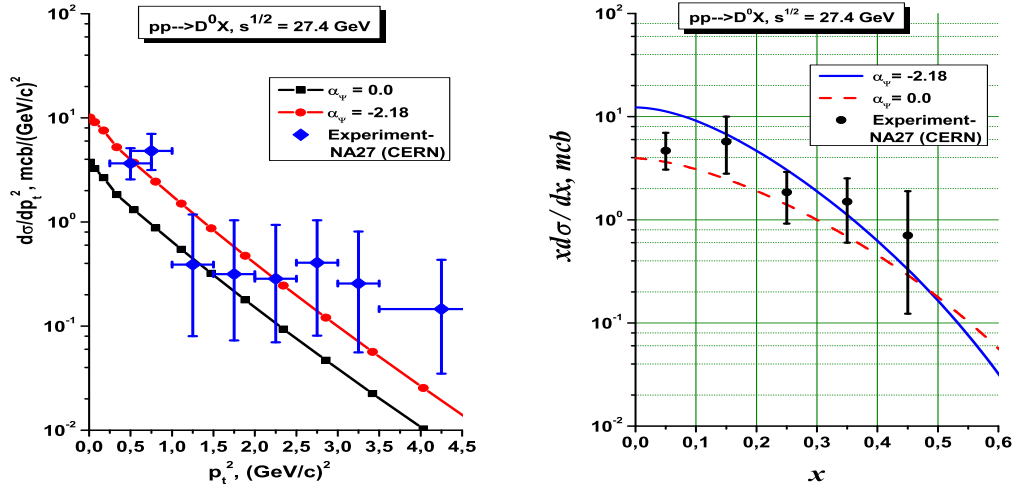


Figure 3: The inclusive spectrum for  $D^0$ -mesons produced in the  $p - p$  collision at  $\sqrt{s} = 27.\text{GeV}$  as a function of  $p_t^2$  (left) and as a function of  $x$  (right), see Refs.[6].

### Acknowledgements

We thank W.Cassing, A.V.Efremov, K.Eggert, D.Elia, A.B.Kaidalov, B.Z.Kopeliovich, A.D.Martin, J.Schukraft, V.V.Uzhinsky and D.Weber for very useful discussions. This work was supported in part by the High Energy Foundation and the World Science Agency and the RFBR grant N 08-02-01003.

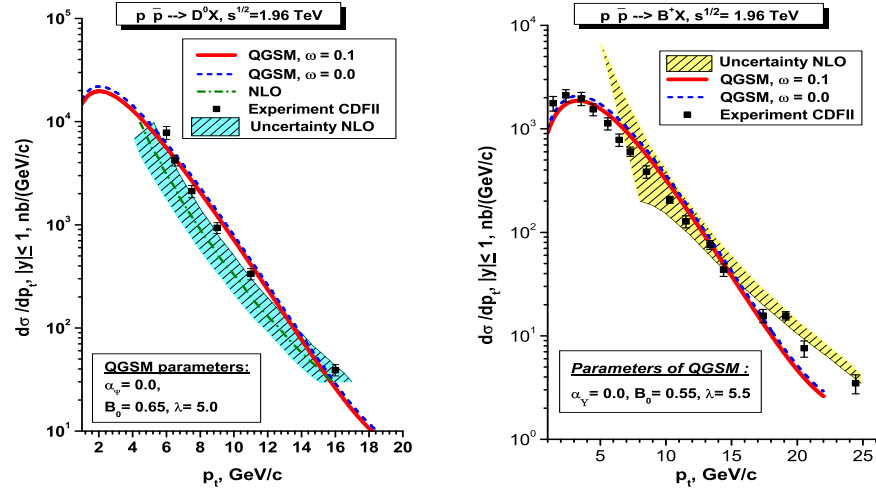


Figure 4: The inclusive  $p_t$ -spectrum for  $D^0$ -mesons (left) and  $B^+$ -mesons (right) produced in the  $p - \bar{p}$  collision at the Tevatron energy  $\sqrt{s} = 1.96$  TeV [12].

## References

- [1] R.D. Field, R.P. Feynman, Phys.Rev. D **15** (1977) 2590; R.D. Field, R.P. Feynman, G.C.Fox, Nucl.Phys. B**128** (1977).
- [2] P. Nason, S. Dawson & R.K. Ellis, Nucl.Phys. B **303** (1988) 607, and B **327** 49 (1989), and B **3335** (1989) 260(E).
- [3] J. Binnewies, B.A. Kniehl & G. Kramer, Phys.Rev. D**58** (1998) 034016.
- [4] A.B. Kaidalov, Phys.Lett. B **116** (1982) 459;  
A.B. Kaidalov, K.A. Ter-Martirosyan, Phys.Lett. B **117** (1982) 247.
- [5] A.B. Kaidalov and O.I.Piskunova, Z.Phys. C**30**, 145 (1986).
- [6] G.I. Lykasov, G.H. Arakelian, M.N. Sergeenko, Phys.Part.Nucl., **30**, 343 (1999);  
G.I. Lykasov, M.N. Sergeenko, Z.Phys. C**70** (1996) 455. *ibid* Z.Phys.C**56**,697 (1992).
- [7] K.A.Ter-Martirosyan, Phys.Lett., B**44**, 377 (1973).



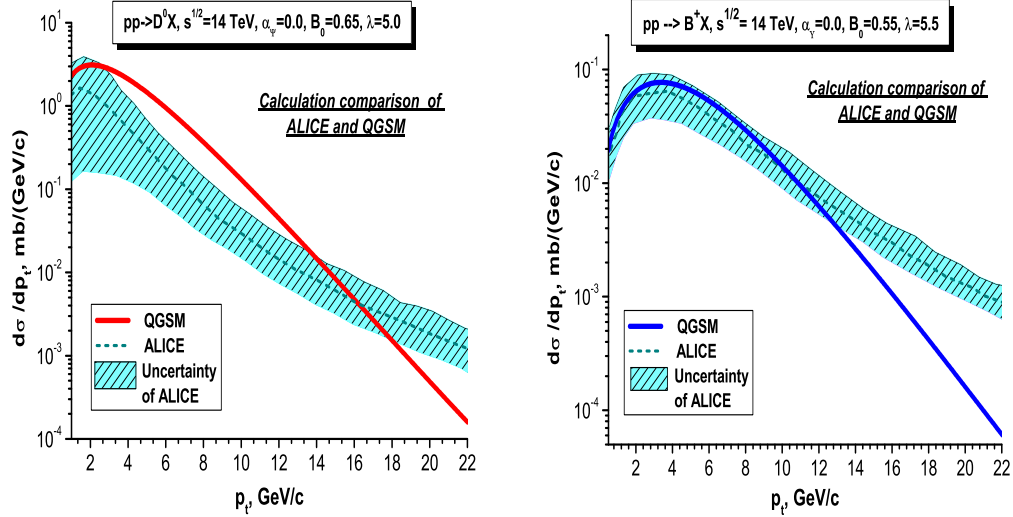


Figure 5: The inclusive spectrum for  $D^0$ -mesons produced in the  $p - p$  collision (left) and the same spectrum for  $B^+$ -mesons (right) at the LHC energy  $\sqrt{s} = 14$  TeV (right) obtained within the QGSM for charmed and beauty mesons and the NLO QCD for  $c$ - and  $b$ -quarks [13].

- [8] NA27 Collaboration, M.Angular-Benitzer, et al., Phys.Lett., **B189**, 476 (1987); *ibid* Phys.Lett., **B201**, 176 (1988).
- [9] V.V.Uzhinsky, A.S.Galoyan, hep-ph/0212369.
- [10] E.Gostman and S.Nussinov, Phys.Rev. **D22**, 624 (1980).
- [11] B.Z.Kopeliovich, B.G.Zakharov, Phys.Lett. **B211**, 221 (1986).
- [12] CDF Collaboration, D. Acosta, *et al.* Phys.Rev.Lett.**91** (2003) 241804.
- [13] ALICE Colaboration, B Alessandro et al., J. Phys. G: Nucl. Part. Phys. **32** (2006) 1295.